# Origin of metallicity of $LaTiO_3/SrTiO_3$ heterostructures

H. Ishida[1] and A. Liebsch[2]
[1]*College of Humanities and Sciences, Nihon University, and CREST JST, Tokyo 156, Japan*
[2]*Institut für Festkörperforschung, Forschungszentrum Jülich, 52425 Jülich, Germany*
(Received 4 November 2007; revised manuscript received 9 January 2008; published 26 March 2008)

It is shown that $LaTiO_3$, in superlattices with $SrTiO_3$, is a strongly correlated metal rather than a Mott insulator. The tetragonal lattice geometry imposed by the $SrTiO_3$ substrate leads to an increase of the Ti $3dt_{2g}$ bandwidth and a reversal of the $t_{2g}$ crystal field relative to the orthorhombic bulk geometry. Using dynamical mean field theory based on finite-temperature multiband exact diagonalization, we show that, as a result of these effects, local Coulomb interactions are not strong enough to induce a Mott transition in tetragonal $LaTiO_3$. The experimentally observed metallicity of $LaTiO_3/SrTiO_3$ heterostructures is therefore caused not only by the interface but also by the tetragonal geometry of the $LaTiO_3$ layers.

DOI: 10.1103/PhysRevB.77.115350 PACS number(s): 73.21.−b, 71.27.+a, 73.40.−c, 78.20.−e

## I. INTRODUCTION

There exists currently considerable interest in the design of nanomaterials with electronic properties that differ qualitatively from those of the constituent components in their bulk form. A particularly intriguing example is the formation of a thin metallic layer at the interface between two insulators. For instance, $SrTiO_3$ is a band insulator with an empty $d$ band, whereas $LaTiO_3$, with one $d$ electron per site, is regarded as a textbook Mott insulator because of strong local Coulomb interactions.[1] Nevertheless, the pioneering work by Ohtomo *et al.*[2] shows that $LaTiO_3/SrTiO_3$ superlattices are metallic, where the overall conductivity depends on the thickness of the $LaTiO_3$ interlayers and on the spacing between them. This phenomenon appears to follow from the fact that the Ti interface layer between adjacent La and Sr planes formally exhibits a $3d^{0.5}$ valency, in contrast to the $3d^1$ and $3d^0$ configurations of bulk $LaTiO_3$ and $SrTiO_3$, respectively. Other examples are $LaAlO_3/SrTiO_3$ heterostructures where a conducting interface was observed although both constituents are wide band gap perovskite insulators.[3] Recently, various other perovskite superlattices have been investigated experimentally.[4–11]

One of the hallmarks of transition metal oxides is their extreme sensitivity to small changes of key parameters such as temperature, pressure, impurity concentration, or structural distortion.[1] The aim of this work is to demonstrate that, as a result of a subtle change of crystal structure, $LaTiO_3$ in superlattices with $SrTiO_3$ is a strongly correlated metal, rather than a Mott insulator such as ordinary bulk $LaTiO_3$. The origin of this symmetry induced insulator to metal transition is that, when $LaTiO_3$ is grown on cubic $SrTiO_3$, the substrate imposes a tetragonal geometry.[12] In contrast, bulk $LaTiO_3$ is orthorhombic. As we show below, this structural modification leads to two significant changes of the electronic properties. First, it causes a substantial increase of the Ti $t_{2g}$ bandwidth. Second, the $t_{2g}$ crystal field is weaker and has the opposite sign compared to bulk $LaTiO_3$. Both effects ensure that the Mott transition in tetragonal $LaTiO_3$ occurs at a significantly larger critical Coulomb energy $U_c$ than in orthorhombic bulk $LaTiO_3$. Thus, for realistic values of $U$, tetragonal $LaTiO_3$ is a strongly correlated metal. $LaTiO_3/SrTiO_3$ superlattices are therefore metal/insulator heterostructures rather than metallic insulator/insulator systems. As a consequence, the metallicity observed in this material is not only induced by the interface layer as believed so far. Instead, it also follows from the metallic nature of tetragonal $LaTiO_3$. These results underline the importance of carefully characterizing the interfaces of superlattices that might be employed in future devices.

The electronic properties of $LaTiO_3/SrTiO_3$ heterostructures have been studied theoretically within a variety of single-electron and many-electron models.[13–21] The conditions under which $LaTiO_3$ in these superlattices might be a Mott insulator, however, have not yet been explored. In view of the striking interplay between Ti $3dt_{2g}$ orbital degrees of freedom and local Coulomb interactions, this issue is crucial and might differ considerably from the situation in bulk $LaTiO_3$. As shown by Pavarini *et al.*,[22] the noncubic octahedral distortions in orthorhombic bulk $LaTiO_3$ give rise to nondiagonal components of the $t_{2g}$ density of states. Nevertheless, from these orbitals, a new basis can be constructed (denoted here as $a_g$, $e_g'$), in which the local density of states is nearly diagonal, and where the $a_g$ contribution lies about 200 meV below the nearly degenerate pair of $e_g'$ components, in agreement with experimental findings.[23] The local Coulomb energy greatly enhances this Ti $3d$ orbital polarization so that for $U \approx 5$ eV a Mott transition occurs where the $a_g$ band is nearly half-filled and the $e_g'$ states are nearly empty.[22] The important conclusion from this picture is that the metal insulator transition in $LaTiO_3$ is intimately connected to the $t_{2g}$ crystal field splitting which reflects, in turn, the orientation and magnitude of the noncubic lattice distortion.

Here, we combine *ab initio* electronic structure calculations for the $SrTiO_3$ induced tetragonal geometry of $LaTiO_3$ with finite-temperature dynamical mean field theory (DMFT)[24,25] and compare the correlated electronic properties with those of the bulk orthorhombic structure. As impurity solver, we use a recent multiband extension[26] of exact diagonalization (ED)[27] which has been shown to be highly useful for the study of strong correlations in several transition metal oxides.[26,28–30] Since this approach does not suffer from sign problems, the full Hund exchange including spin-flip and pair-exchange contributions can be taken into account. Also,

 

relatively large Coulomb energies and low temperatures can be reached. These DMFT results demonstrate that the metallic or insulating nature of $LaTiO_3$ depends sensitively on the interplay between lattice geometry and orbital degrees of freedom, in particular, on the sign and magnitude of the crystal field splitting between $t_{2g}$ orbitals.

This paper is organized as follows. In the next section, we give the details concerning the evaluation of the one-electron properties of $LaTiO_3$ in the tetragonal geometry and specify the main aspects of the many-body calculations that account for strong local Coulomb correlations at Ti sites. Section III contains the results and discussion. Finally, Sec. IV provides the conclusion.

## II. CALCULATIONAL DETAILS

To illustrate the effect of changing the lattice structure of $LaTiO_3$ from orthorhombic to tetragonal, we have studied two cases. First, we consider a hypothetical bulk geometry where the lattice constant in the $xy$ plane is fixed to that of $SrTiO_3$, with $a=b=3.92$ Å. The lattice parameter in the $z$ direction was optimized by minimization of the total energy. We have used the Vienna *ab initio* simulation package (VASP)[31] which represents an implementation of the projector augmented-wave method.[32] The total energy of the system was calculated within the nonspin-polarized generalized gradient approximation.[33] We assumed a $1\times1$ geometry without considering rotation and tilting of $TiO_6$ octahedra. The resulting spacing $c=4.01$ Å is only slightly smaller than $c=4.106$ Å obtained for a tetragonal lattice with the same unit cell volume as in the orthorhombic case.

The second calculation is for a $(LaTiO_3)_3/(SrTiO_3)_4$ superlattice containing five Ti layers with only La neighboring planes (nominal $d^1$ configuration), three Ti layers with only Sr neighboring planes (nominal $d^0$ configuration), and two Ti interface layers with La and Sr neighboring planes (nominal $d^{0.5}$ configuration). The lateral structure in the $xy$ plane was again assumed to be the same as for $SrTiO_3$, but the interlayer spacings in the $z$ direction were optimized by minimizing the total energy. For each optimized geometry, we performed a local density approximation (LDA) calculation of states using a home-made full-potential linearized augmented plane wave (FLAPW) code to evaulate the partial density of states projected on Ti $3d$ orbitals in muffin-tin spheres.

In the ED/DMFT scheme, each of the three $t_{2g}$ orbitals (i.e., $d_{xy}$, $d_{xz,yz}$ for the tetragonal lattice and $a_g$, $e_g'$ for orthorhombic $LaTiO_3$) couples to two or three bath levels, giving a cluster size $n_s=9$ or $n_s=12$. In the tetragonal structure, local quantities such as the impurity Green's function and self-energy are diagonal in the $d_{xy}$, $d_{xz,yz}$ representation. In the bulk orthorhombic case, hybridization between $a_g$, $e_g'$ orbitals is very small. We therefore neglect nondiagonal density components in this basis, so that the Green function and self-energy are also diagonal in this representation. Also, the small difference between the $e_g'$ densities is omitted and their average density is used instead. The cluster Hamiltonian is given by

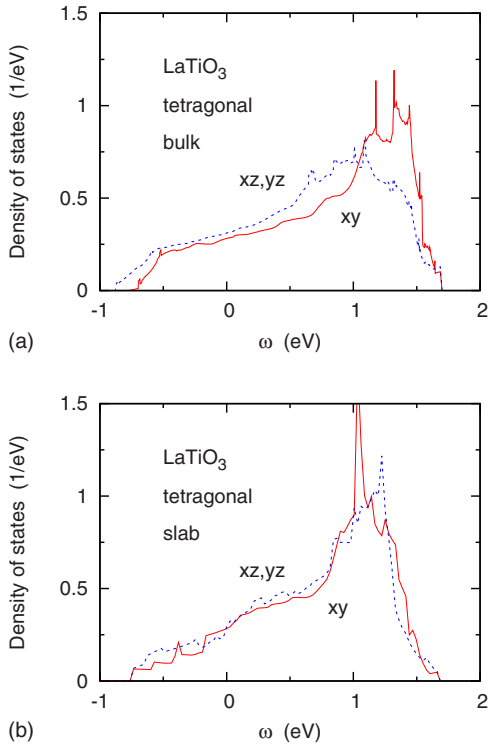


FIG. 1. (Color online) Upper panel: $t_{2g}$ density of states components of $LaTiO_3$ in hypothetical tetragonal bulk geometry. Solid (red) curve: $d_{xy}$ states; dashed (blue) curves: $d_{xz,yz}$ states. $E_F=0$. Lower panel: analogous density of states components for central Ti atom in $(LaTiO_3)_6/(SrTiO_3)_4$ superlattice, assuming unit occupancy (see text).

$$H=\sum_{m\sigma}(\varepsilon_m-\mu)n_{m\sigma}+\sum_{k\sigma}\varepsilon_k n_{k\sigma}+\sum_{mk\sigma}V_{mk}[c_{m\sigma}^{+}c_{k\sigma}+\text{H.c.}]$$
$$+\sum_{m}Un_{m\uparrow}n_{m\downarrow}+\sum_{m<m'\sigma\sigma'}(U'-J\delta_{\sigma\sigma'})n_{m\sigma}n_{m'\sigma'}$$
$$-\sum_{m\neq m'}J[c_{m\uparrow}^{+}c_{m\downarrow}c_{m'\downarrow}^{+}c_{m'\uparrow}+c_{m\uparrow}^{+}c_{m\downarrow}^{+}c_{m'\uparrow}c_{m'\downarrow}],$$

where $\varepsilon_{m=1,\ldots,3}$ and $\varepsilon_{k=4,\ldots,n_s}$ are the impurity and bath levels, respectively, $V_{mk}$ the hybridization matrix elements, and $\mu$ is the chemical potential. $U$, $U'$, and $J$ are the on-site Coulomb and exchange energies, with $U'=U-2J$. Only paramagnetic phases are considered. For further details, see Ref. 26.

## III. RESULTS AND DISCUSSION

The upper panel of Fig. 1 shows the Ti $t_{2g}$ density of states components for the hypothetical tetragonal bulk geometry of $LaTiO_3$. In this symmetry, the singly degenerate $d_{xy}$ density differs from the doubly degenerate $d_{xz,yz}$ distributions. The overall width of the $t_{2g}$ bands is about $W_{\text{tetra}}\approx2.5$ eV, where we have neglected small additional spectral weight in the region of the empty $e_g$ bands at higher energies. Also, the centroid of the $d_{xy}$ band is seen to lie above that of the $d_{xz,yz}$ bands. As a result of this *positive* crystal field splitting, the subband occupancies (per spin band) for the tetragonal bulk are $n_{xy}\approx0.14$ and $n_{xz,yz}\approx0.18$.

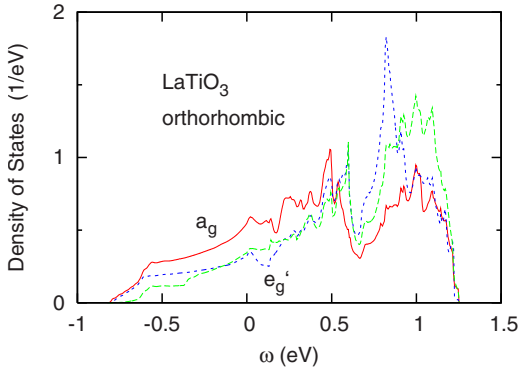


FIG. 2. (Color online) Density of states components of orthorhombic bulk $LaTiO_3$ in nearly diagonal subband representation (Ref. 22). Solid (red) curve: $a_g$ states; dashed (blue and green) curves: $e_g'$ states. $E_F=0$.

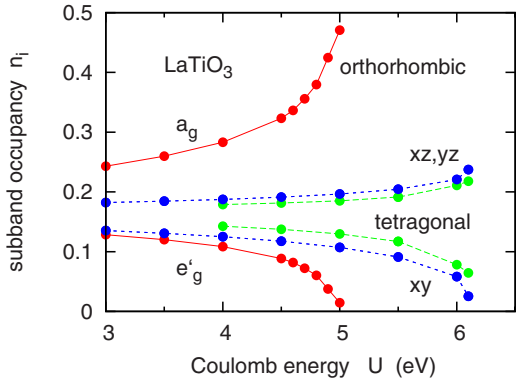


FIG. 3. (Color online) Ti $3d$ subband occupancies of $LaTiO_3$ as a function of the local Coulomb energy. Solid (red) curves: orthorhombic bulk geometry, indicating metal insulator transition at $U \approx 5$ eV. Short-dashed (blue) curves: tetragonal bulk geometry; long-dashed (green) curves: tetragonal slab geometry, both for integer occupancy. Since the crystal field splitting has opposite sign in the orthorhombic and tetragonal structures, the orbital polarization between singly degenerate $a_g$ $(d_{xy})$ and doubly degenerate $e_g'$ $(d_{xz,yz})$ states is reversed.

In the experimental work of Ohtomo *et al.*,[2] rather thin $LaTiO_3$ layers containing up to five La planes were studied. The lower panel of Fig. 1 shows the $t_{2g}$ density of states components for a $(LaTiO_3)_6/(SrTiO_3)_4$ superlattice, containing five Ti layers with La neighboring planes, as specified in the preceding section. Plotted is the density of states for the central Ti atom within the $LaTiO_3$ slab, assuming integer occupancy (see below). The vertical height of the $O_6$ octahedron surrounding this atom, 3.98 Å, is slightly smaller than that in the tetragonal bulk, 4.01 Å. As a result, the difference between the $d_{xy}$ and $d_{xz,yz}$ densities is even smaller than that in bulk case shown in the upper panel of Fig. 1. Thus, the $t_{2g}$ shell at the central Ti atom is slightly more isotropic than for the tetragonal bulk.

For comparison, we show in Fig. 2 the $a_g$ and $e_g'$ densities of orthorhombic bulk $LaTiO_3$, which are obtained from a linear transformation of the original Ti $d_{xy,xz,yz}$ orbitals.[22] As mentioned above, in the $a_g$, $e_g'$ basis, the orthorhombic density of states is nearly diagonal and the centroid of the $a_g$ density lies about 200 meV below the two $e_g'$ components, implying a *negative* crystal field splitting between the singly and doubly degenerate densities. The subband occupancies (per spin band) are $n_{a_g} \approx 0.23$ and $n_{e_g'} \approx 0.135$. Thus, orbital polarization is much larger than for the tetragonal structures shown in Fig. 1 and has the opposite sign. Moreover, the width of the $a_g$, $e_g'$ bands, $W_{\text{ortho}} \approx 2$ eV, is considerably smaller than in the tetragonal case. On the whole, therefore, the noncubic distortions are significantly smaller for the tetragonal interlayer structure than for the orthorhombic bulk form of $LaTiO_3$. This difference is also apparent in the shape of the density of states since the tetragonal distributions shown in Fig. 1 resemble more closely the characteristic $t_{2g}$ density of cubic $SrVO_3$ (width $W_{\text{cubic}}=2.8$ eV).[22]

In the case of the tetragonal and orthorhombic bulk structures, the Ti $t_{2g}$ shell has a $3d^1$ configuration. In the tretragonal slab geometry, part of the $LaTiO_3$ valence charge spreads into the $SrTiO_3$ layers, thereby reducing the $t_{2g}$ occupancy in the $LaTiO_3$ region below unity. To estimate the layer dependence of these $t_{2g}$ occupancies, we multiply the $t_{2g}$ charge calculated in a Ti muffin-tin sphere ($R=2.18$ a.u.) of each layer by a constant, such that the total charge becomes six, as required for a $(LaTiO_3)_6/(SrTiO_3)_4$ superlattice. This procedure is approximate since it assumes that the muffin-tin charge is representative of the $t_{2g}$ charge in the interstitial region. Nevertheless, it may be useful for a qualitative estimate of the occupancies. The charge variation from the central Ti atom in the La film to the central Ti atom in the Sr layer is then given by $n=0.809$, 0.819, 0.739, 0.516, 0.335, and 0.373, where $n=0.516$ corresponds to the Ti interface atom. These results are for relaxed layer spacings. Without lattice relaxation, the corresponding occupancies are $n=1.118$, 1.044, 0.978, 0.335, 0.067, and 0.030, where $n=0.335$ corresponds to the interface plane. Thus, in agreement with previous works,[16,17] the occupancies in the interior of the $SrTiO_3$ slab are greatly enhanced by the lattice relaxation, i.e., by allowing the layer spacing in the superlattice to be energetically optimized. The important point of these results is that the $3d$ occupancies in the interior of the relaxed $LaTiO_3$ slab differ appreciably from unity. As will be discussed below, this deviation from integer occupancy further enhances the metallicity of the superlattice.

We first show now that, as a result of the wider bandwidth, the weaker orbital polarization, and the opposite sign of this polarization, $LaTiO_3$ in the tetragonal bulk geometry is a strongly correlated metal, rather than a Mott insulator as in the usual orthorhombic bulk form. To evaluate the electronic properties of $LaTiO_3$ in the presence of strong local Coulomb interactions, we use multiband ED/DMFT.[26] Full Hund exchange is included, with the exchange energy $J=0.65$ eV held fixed at the value appropriate for the bulk material.[22] To locate the Mott transition, the intraorbital Coulomb energy $U$ is varied, and the interorbital Coulomb interaction is given by $U'=U-2J$. The temperature is $T=20$ meV.

Figure 3 shows the subband occupancies as a function of Coulomb energy. For the orthorhombic geometry, nearly complete orbital polarization between $a_g$ and $e_g'$ states is reached at about $U=5$ eV, which agrees with previous DMFT results using the quantum Monte Carlo technique as

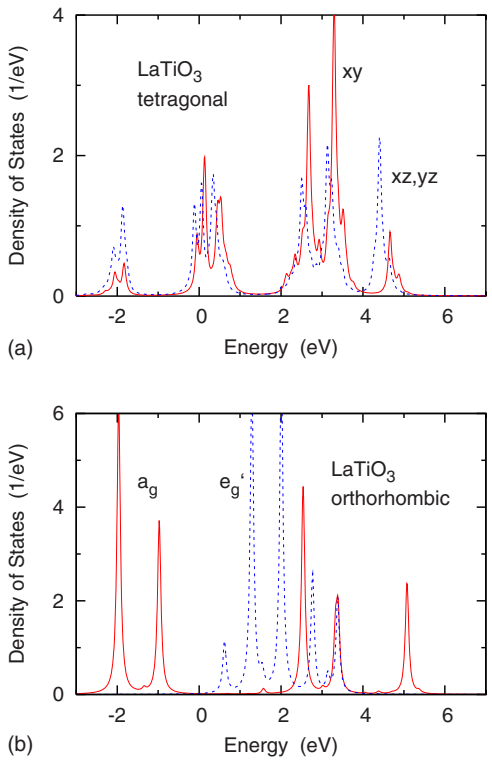


FIG. 4. (Color online) $LaTiO_3$ $3dt_{2g}$ spectral distributions. Upper panel: tetragonal bulk geometry, $U=5.5$ eV, indicating strongly correlated metallic behavior. Lower panel: orthorhombic bulk geometry, $U=5$ eV, indicating the Mott insulating behavior. Solid (red) curves: singly degenerate $d_{xy}$ ($a_g$) states; dashed (blue) curves: doubly degenerate $d_{xz,yz}$ ($e_g'$) states. $E_F=0$.

impurity solver.[22] The spectral distributions (see Fig. 4) show that the nearly half-filled $a_g$ band then consists of lower and upper Hubbard peaks whereas the $e_g'$ bands are pushed above the Fermi level.[22,30]

In the case of the tetragonal bulk structure, the situation is qualitatively different since the crystal field is weaker and has opposite sign. As shown in Fig. 3, now the enhancement of the orbital polarization via the Coulomb interaction implies that the $d_{xy}$ band is pushed above the Fermi level and that the degenerate $d_{xz,yz}$ bands are driven to 1/4 occupancy. As a result of this reversal of crystal field, and because of its weaker magnitude (i.e., weaker orbital polarization in the uncorrelated limit), the metal insulator transition occurs above $U=6$ eV. Since the local Coulomb energy for Ti is approximately 5 eV,[22] this result implies that in the tetragonal bulk geometry, $LaTiO_3$ is on the metallic side of the Mott transition. As mentioned above, we have neglected small contributions to the tetragonal density of states in the region of the empty $e_g$ bands. Inclusion of these states would increase the tetragonal $t_{2g}$ bandwidth and reinforce the metallic behavior.

To illustrate the effect of the slab geometry on the $LaTiO_3$ Mott transition, we also show in Fig. 3 the subband occupancies for the central Ti layer under the assumption of integer occupancy. Compared to the tetragonal bulk structure, the transition is seen to be shifted to even larger $U$. This is a consequence of the weaker orbital polarization associated with the smaller deviations of the density of states components from cubic symmetry, as is evident also from the results shown Fig. 1.

In Fig. 4, we compare the $LaTiO_3$ $t_{2g}$ spectral distributions for the tetragonal and orthorhombic bulk crystal structures. Since we are concerned here only with the difference between metallic and insulating behavior, it is sufficient to use the ED cluster spectra which can be evaluated at real $\omega$, without requiring extrapolation from the imaginary Matsubara frequencies. In the orthorhombic case, the system is already insulating at $U=5$ eV, with an excitation gap formed between the lower Hubbard peak of the $a_g$ band and the empty $e_g'$ bands, in agreement with Ref. 22. The tetragonal geometry, on the other hand, is still metallic at $U=5.5$ eV, with conduction states near $E_F$ arising from $d_{xy}$ and $d_{xz,yz}$ bands.

The important consequence of the above results is that $LaTiO_3/SrTiO_3$ heterostructures are metal/insulator rather than insulator/insulator superlattices. The observed metallicity therefore originates in the basic electronic properties of the tetragonal $LaTiO_3$ layer, instead of being driven by the metallic interface between a Mott insulator and a band insulator. In the remainder of this section, we argue that this metallic behavior is further reinforced by the spreading of the $LaTiO_3$ valence charge into the adjacent $SrTiO_3$ layer.

As pointed out above, the leakage of the $LaTiO_3$ $t_{2g}$ states into $SrTiO_3$ reduces the on-site $3d$ occupancy below unity. Thus, the effectively hole doped electronic system in the $LaTiO_3$ layer is even farther removed from the Mott transition which would occur above $U=6$ eV at integer occupancy (see Fig. 3). The same effect occurs, of course, if the $LaTiO_3$ layers are assumed to have orthorhombic symmetry. As a result of the local Coulomb interactions, the layer dependent $3d$ occupancies might differ slightly from the LDA values quoted above. This effect could, in principle, be estimated by performing coupled DMFT calculations, in analogy to earlier work for one-band models of heterostructures[13,19,21] and bare surfaces.[34] For the present multiband system, such a calculation is beyond the scope of this paper. It is clear, however, that the overall metallicity of the $LaTiO_3/SrTiO_3$ superlattice results from two sources: the tetragonal $LaTiO_3$ geometry and the noninteger occupancies of the Ti $t_{2g}$ shells. Because of the near one-half occupancy of the interface layers, they are likely to be less correlated than the inner Ti planes. As a result, they might contribute more strongly to the overall metallicity observed in the experiments.[2,35]

## IV. CONCLUSION

In summary, we have shown that in $LaTiO_3/SrTiO_3$ superlattices, the change from orthorhombic to tetragonal crystal structure enforced by the $SrTiO_3$ substrate causes a fundamental change in the electronic properties of $LaTiO_3$. Instead of being a Mott insulator as in the usual bulk geometry, tetragonal $LaTiO_3$ is a highly correlated metal. Thus, the metallicity observed in these heterostructures is not only caused by the noninteger $3d$ occupancy of Ti ions at the interface. It is also a consequence of the tetragonal $LaTiO_3$ geometry imposed by the $SrTiO_3$ substrate. It would be very

interesting to use transmission electron microscopy to determine the $LaTiO_3$ layer thickness at which the orthorhombic structure begins to be energetically favorable. The Mott insulating behavior should then emerge in the central regions of these $LaTiO_3$ layers at sufficiently large thickness.

The above results demonstrate the extreme sensitivity of the electronic properties of perovskites to small changes in key parameters. In the present case, the slightly modified crystal structure caused by the deposition of $LaTiO_3$ onto $SrTiO_3$ gives rise to a subtle but important change in its single-electron spectral distribution, which, in turn, has a profound effect on the properties of the correlated electron system. For an adequate interpretation of experimental data, it is therefore of great importance to have accurate structural information. On the theoretical side, it is crucial to include the full details of the single-particle electronic properties for a given lattice geometry and to account for the orbital degrees of freedom in the multiband many-body calculation.

## ACKNOWLEDGMENTS

We would like to thank Eva Pavarini for the density of states shown in Fig. 2, and S. S. A. Seo and T. W. Noh for comments.

[1] M. Imada, A. Fujimori, and Y. Tokura, Rev. Mod. Phys. **70**, 1039 (1998).
[2] A. Ohtomo, D. A. Muller, J. L. Grazul, and H. Y. Hwang, Nature (London) **419**, 378 (2002).
[3] A. Ohtomo and H. Y. Hwang, Nature (London) **427**, 423 (2004).
[4] M. Takizawa, H. Wadati, K. Tanaka, M. Hashimoto, T. Yoshida, A. Fujimori, A. Chikamatsu, H. Kumigashira, M. Oshima, K. Shibuya, T. Mihara, T. Ohnishi, M. Lippmaa, M. Kawasaki, H. Koinuma, S. Okamoto, and A. J. Millis, Phys. Rev. Lett. **97**, 057601 (2006).
[5] L. F. Kourkoutis, Y. Hotta, T. Susaki, H. Y. Hwang, and D. A. Muller, Phys. Rev. Lett. **97**, 256803 (2006).
[6] K. Maekawa, M. Takizawa, H. Wadati, T. Yoshida, A. Fujimori, H. Kumigashira, M. Oshima, Y. Muraoka, Y. Nagao, and Z. Hiroi, Phys. Rev. B **76**, 115121 (2007).
[7] H. Wadati, Y. Hotta, A. Fujimori, T. Susaki, H. Y. Hwang, Y. Takata, K. Horiba, M. Matsunami, S. Shin, M. Yabashi, K. Tamasaku, Y. Nishino, and T. Ishikawa, Phys. Rev. B **77**, 045122 (2008).
[8] S. J. May, S. G. E. te Velthuis, M. R. Fitzsimmons, X. Zhai, J. N. Eckstein, S. D. Bader, and A. Bhattacharya, arXiv:0709.1715 (unpublished).
[9] A. Bhattacharya, S. J. May, S. G. E. te Velthuis, M. Warusawithana, X. Zhai, A. B. Shah, J.-M. Zuo, M. R. Fitzsimmons, S. D. Bader, and J. N. Eckstein, arXiv:0710.1452 (unpublished).
[10] Y. Hotta, T. Susaki, and H. Y. Hwang, arXiv:0710.2174 (unpublished).
[11] W. C. Sheets, B. Mercey, and W. Prellier, Appl. Phys. Lett. **91**, 192102 (2007).
[12] K. H. Kim, D. P. Norton, J. D. Budai, M. F. Chisholm, B. C. Sales, D. K. Christen, and C. Cantoni, Phys. Status Solidi A **200**, 346 (2003).
[13] S. Okamoto and A. J. Millis, Nature (London) **427**, 630 (2004); Phys. Rev. B **70**, 075101 (2004); **70**, 241104(R) (2004); **72**, 235108 (2005).
[14] J. K. Freericks, Phys. Rev. B **70**, 195342 (2004).
[15] Z. S. Popovic and S. Satpathy, Phys. Rev. Lett. **94**, 176805 (2005).
[16] S. Okamoto, A. J. Millis, and N. A. Spaldin, Phys. Rev. Lett. **97**, 056802 (2006).
[17] D. R. Hamann, D. A. Muller, and H. Y. Hwang, Phys. Rev. B **73**, 195403 (2006).
[18] W.-C. Lee and A. H. MacDonald, Phys. Rev. B **74**, 075106 (2006); arXiv:0708.0554 (unpublished).
[19] S. S. Kancharla and E. Dagotto, Phys. Rev. B **74**, 195427 (2006).
[20] P. G. Silvestrov and K. B. Efetov, Phys. Rev. Lett. **98**, 016802 (2007).
[21] A. Rüegg, S. Pilgram, and M. Sigrist, Phys. Rev. B **75**, 195117 (2007).
[22] E. Pavarini, S. Biermann, A. Poteryaev, A. I. Lichtenstein, A. Georges, and O. K. Andersen, Phys. Rev. Lett. **92**, 176403 (2004); E. Pavarini, A. Yamasaki, J. Nuss, and O. K. Andersen, New J. Phys. **7**, 188 (2005).
[23] M. Cwik, T. Lorenz, J. Baier, R. Muller, G. Andre, F. Bouree, F. Lichtenberg, A. Freimuth, R. Schmitz, E. Müller-Hartmann, and M. Braden, Phys. Rev. B **68**, 060401(R) (2003); M. W. Haverkort, Z. Hu, A. Tanaka, G. Ghiringhelli, H. Roth, M. Cwik, T. Lorenz, C. Schussler-Langeheine, S. V. Streltsov, A. S. Mylnikova, V. I. Anisimov, C. de Nadai, N. B. Brookes, H. H. Hsieh, H.-J. Lin, C. T. Chen, T. Mizokawa, Y. Taguchi, Y. Tokura, D. I. Khomskii, and L. H. Tjeng, Phys. Rev. Lett. **94**, 056401 (2005).
[24] W. Metzner and D. Vollhardt, Phys. Rev. Lett. **62**, 324 (1989); E. Müller-Hartmann, Z. Phys. B: Condens. Matter **74**, 507 (1989); A. Georges and G. Kotliar, Phys. Rev. B **45**, 6479 (1992); M. Jarrell, *ibid.* **69**, 168 (1992).
[25] A. Georges, G. Kotliar, W. Krauth, and M. J. Rozenberg, Rev. Mod. Phys. **68**, 13 (1996).
[26] C. A. Perroni, H. Ishida, and A. Liebsch, Phys. Rev. B **75**, 045125 (2007); See also A. Liebsch, Phys. Rev. Lett. **95**, 116402 (2005); A. Liebsch and T. A. Costi, Eur. Phys. J. B **51**, 523 (2006).
[27] M. Caffarel and W. Krauth, Phys. Rev. Lett. **72**, 1545 (1994).
[28] A. Liebsch and H. Ishida, Phys. Rev. Lett. **98**, 216403 (2007).
[29] A. Liebsch and H. Ishida, Eur. Phys. J. B **61**, 405 (2008).
[30] A. Liebsch, Phys. Rev. B **77**, 115115 (2008).
[31] G. Kresse and J. Furthmüller, Comput. Mater. Sci. **6**, 15 (1996), and references therein.
[32] P. E. Blöchl, Phys. Rev. B **50**, 17953 (1994).
[33] J. P. Perdew and Y. Wang, Phys. Rev. B **45**, 13244 (1992).
[34] S. Schwieger, M. Potthoff, and W. Nolting, Phys. Rev. B **67**, 165408 (2003), and references therein.
[35] S. S. A. Seo, W. S. Choi, H. N. Lee, L. Yu, K. W. Kim, C. Bernhard, and T. W. Noh, Phys. Rev. Lett. **99**, 266801 (2007).